J Am Oil Chem Soc (2019)
DOI 10.1002/aocs.12229

ORIGINAL ARTICLE

Solvent-Free Enzymatic Synthesis of 1-*o*-Galloylglycerol Optimized by the Taguchi Method

Siyu Zhang[1] · **Casimir C. Akoh**[1]

Received: 21 February 2019 / Revised: 17 April 2019 / Accepted: 24 April 2019

Abstract Gallic acid (GA) and its lipophilic forms, alkyl gallates, have been widely used in several industrial fields as antioxidants. However, the potential harmful effects of alkyl gallates, such as estrogenic effects, limit their application and raise safety concerns. The glycerol ester of GA, 1-*o*-galloylglycerol (GG), has not been reported to cause adverse health effects. Owing to the steric and electron-donating effects of GA, lipase-catalyzed synthesis of GG has not been successfully achieved. In this work, glycerol ester of GA, GG, was successfully synthesized for the first time by the enzymatic transesterification of glycerol and *n*-propyl gallate (PG). GG was synthesized with an immobilized and commercially available food-grade lipase (Lipozyme® 435) under solvent-free (no extra solvent) conditions at atmospheric pressure and nitrogen flow. The effects of the reaction conditions, including the reaction temperature, substrate molar ratio, reaction time, and enzyme load, were optimized using the Taguchi method and regression analysis. The structure of the product was elucidated using Fourier-transform infrared spectroscopy (FT-IR), electrospray ionization high-resolution accurate-mass tandem mass spectrometry (ESI-HRAM-MS/MS), and 1D and 2D nuclear magnetic resonance spectroscopy (NMR). Under the optimal conditions, GG was synthesized in 67.1 ± 1.9% yield at 50°C, 25:1 (glycerol:PG) substrate molar ratio, 120 hours, and 23.8% enzyme load relative to the total weight of the substrates.

Keywords 1-*o*-galloylglycerol · lipase-catalyzed alcoholysis · solvent-free · Taguchi method

✉ Casimir C. Akoh
cakoh@uga.edu

[1] Department of Food Science & Technology, University of Georgia, Athens, GA 30602, USA

Introduction

Gallic acid (GA) is a natural phenolic compound that is abundant in various plants, such as tea leaves, gallnuts, hazelnuts, and grapes (Masoud et al., 2012). It is a phenolic secondary metabolite that functions as an antioxidant in plants. Antioxidants are important components of food, cosmetic, and pharmaceutical products, because they slow down the oxidation of unsaturated lipids and the associated generation of unpleasant flavors, thereby preserving product quality. The widely used synthetic antioxidants in food products, such as butylated hydroxyanisole (BHA), butylated hydroxytoluene (BHT), tert-butyl hydroquinone (TBHQ), and alkyl esters of GA, are suspected of being carcinogenic (BHA, BHT, and TBHQ) (Stamatis et al., 1999) and contact allergenic/estrogenic (alkyl esters of GA) (Gamboni et al., 2013; Ter Veld et al., 2006). The interest in using natural antioxidants, such as GA, is increasing owing to the potential beneficial effects against inflammatory and cardiovascular diseases as well as neuroprotective effects (Locatelli et al., 2013; Nayeem and Smb, 2016). However, the application of GA as an antioxidant has been limited because of its poor solubility in aqueous and nonpolar media.

As a hydroxybenzoic acid derivative, the solubility of GA in both aqueous and nonpolar media is not satisfactory, which limits its effectiveness in water/oil systems. GA is basically insoluble in oil and fat, whereas the solubility of GA in water is highly dependent on the temperature and requires a long time (4 hours) to reach equilibrium at room temperature (Daneshfar et al., 2008). Glycosylation and

lipophilization are two methods that have been proposed to solve the solubility problem of GA in aqueous and oil systems, respectively (Nam et al., 2017; Otto et al., 2000). However, their products may not be suitable for use as common antioxidants in food products. For example, β-glucogallin, the glycosylation product of GA, is an aldose reductase inhibitor, which is a medicine for diabetic eye disease (Puppala et al., 2012). As products of the lipophilization of GA, alkyl gallates may have an estrogenic effect by acting as antagonists of estrogen-response elements; such an effect is associated with the chain length of the alkyl group (Ter Veld et al., 2006). Moreover, numerous studies have indicated that alkyl gallates could cause contact dermatitis and stomatitis (Gamboni et al., 2013). Furthermore, alkyl gallates are susceptible to hydrolysis during digestion, releasing alkyl alcohol in the gastrointestinal tract (EFSA Panel on Food Additives and Nutrient Sources Added to Food, 2014), which could be a health concern.

The glycerol ester of GA, 1-*o*-galloylglycerol (GG), could be a better alternative to both β-glucogallin and alkyl gallates. As a glycerol monoester, GG is not only readily soluble in aqueous media, it can also be transformed into a lipophilic form through well-established chemical or new enzymatic esterification to esterify one or two of the remaining hydroxyl groups with fatty acid(s) (Sun et al., 2015). Even without further modification, GG could be directly used in vegetable oil products and has a better antioxidant effect than propyl gallate (PG) and BHT (Song and Xiao, 1988). GG has not been reported to have any adverse health effects and would only release glycerol aside from GA during digestion, which is much less toxic than alkyl alcohol (released from alkyl gallates during digestion). Furthermore, the gastrointestinal side effect of GA could be avoided by esterification of the carboxylic acid group (Ravelo et al., 2016). Notably, GG is a natural component of many plants, such as *Rheum rhabarbarum* (Nonaka and Nishioka, 1983). However, the natural occurrence of GG is low. An efficient synthesis method for GG is necessary for its potential application in the food, pharmaceutical, and cosmetic industries.

The synthesis of GG was first achieved by chemical synthesis (Artamonov et al., 1999; Nonaka and Nishioka, 1983; Song and Xiao, 1988). The chemical synthesis of GG involves multiple protection steps of the hydroxyl groups in both glycerol and GA, and the yield of GG was less than 70% (Song and Xiao, 1988). Without protecting the hydroxyl groups, the yield of GG in the transesterification reaction of methyl gallate and glycerol was less than 12% (Artamonov et al., 1999). Although they are simple and rapid, chemical reactions are nonselective and result in unwanted by-products, in turn leading to low yields and the need for complex purification steps (Roby, 2017). In contrast, the enzyme selectivity minimizes the side reactions and limits the formation of by-products, which leads to high purity of the reaction products, fewer reaction intermediates and purification steps, and a more environmentally friendly and green reaction route (Figueroa-Espinoza et al., 2013). Although the reaction time is usually longer, the cost of using enzymes is higher, and inhibition/deactivation issues related to the reaction conditions need to be considered, enzymatic reaction is still the best choice for meeting the stringent requirements that are necessary for food applications (Buisman et al., 1998).

The enzymatic synthesis of GG is limited due to the steric hindrance and electrostatic interaction between the bulky phenyl ring of GA and the active site of the enzyme, like some lipases (Tamayo et al., 2012). The enzymatic syntheses of the glycerol esters of benzoic, ferulic, caffeic, and 3,4-dihydroxyphenylacetic acids, and ibuprofen have been achieved in recent years (Compton et al., 2000; Ravelo et al., 2016; Sun and Hu, 2017; Tamayo et al., 2012). Particularly, the synthesis and application of the glycerol esters of ferulic acid have been extensively studied. Not only 1-feruloyl-*sn*-glycerol, but glyceryl diferulate, feruloyl monoacylglycerol, feruloyl diacylglycerol, and glyceryl triferulate have also been successfully synthesized for use as antioxidants (Compton et al., 2012; Hollande et al., 2018; Sun et al., 2015), as building blocks for polymer chemistry (Pion et al., 2013), or sunscreen ingredients (Compton et al., 2000), in ionic liquids, hydrophobic solvents, and under solvent-free conditions. Because of the structure of GA, its enzymatic esterification by commercially available enzymes was considered unfeasible (Figueroa-Espinoza et al., 2013; Figueroa-Espinoza and Villeneuve, 2005; Otto et al., 2000). To our knowledge, the enzymatic synthesis of GG has not yet been achieved before. *Candida antarctica* lipase B (CALB) has a funnel-like active center with a very short lid, which is similar to esterases, and is inclined to adapt to more voluminous acids such as benzoic acid and its derivatives (Tamayo et al., 2012). Lipozyme® 435 is a commercially available food-grade immobilized form of CALB (Willett and Akoh, 2018). It has high thermostability and is capable of catalyzing reaction in a solvent or in solvent-free media (Willett and Akoh, 2018). Based on its properties, Lipozyme® 435 appears to be a good choice for enzymatically synthesizing GG for use in food products.

Herein, we report an efficient enzymatic synthesis method for producing GG catalyzed by a commercially available food-grade enzyme in solvent-free media under atmospheric pressure. As depicted in Scheme 1, alcoholysis (transesterification) of PG with glycerol is proposed as the route of synthesis. The Taguchi method (Taguchi, 1987) and regression analysis were used to optimize the synthesis conditions, including the reaction temperature, substrate ratio, reaction time, and enzyme load. The structure of the

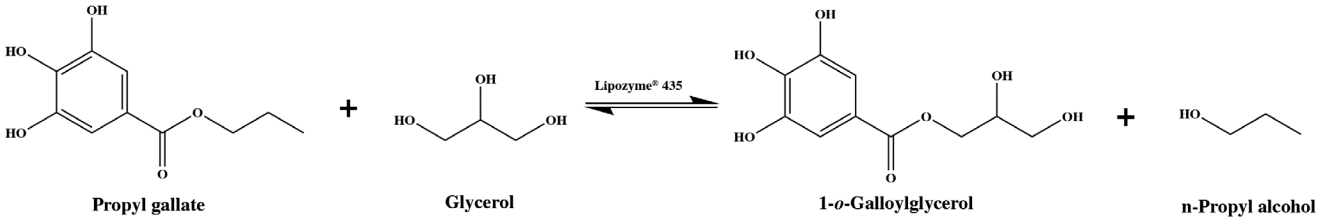

Scheme 1 Synthesis of GG based on the alcoholysis of PG with glycerol

product was determined by Fourier-transform infrared spectroscopy (FT-IR), electrospray ionization high-resolution accurate-mass tandem mass spectrometry (ESI-HRAM-MS/MS), and 1D and 2D nuclear magnetic resonance spectroscopy (NMR).

Materials and Methods

Chemicals and Reagents

n-Propyl gallate (≥98%) was purchased from HiMedia Laboratories (Nashik, India). Glycerol was purchased from Hoefer Inc. (San Francisco, CA, US). Lipozyme® RM IM (lipase from *Rhizomucor miehei*, immobilized on an anionic exchange resin, with specific activity of 442 interesterification unit g^{-1}), Lipozyme® TL IM (lipase from *Thermomyces lanuginosus* and immobilized on a noncompressible silica gel carrier, with specific activity of 250 interesterification unit g^{-1}), Novozym® 435 (lipase B from *Candida antarctica*, immobilized on a macroporous acrylic resin, with specific activity of 10,000 propyl laurate unit g^{-1}), and Lipozyme® 435, a food-grade lipase (recombinant lipase B from *C. antarctica*, expressed in *Aspergillus niger*, and immobilized on a macroporous hydrophobic resin, with specific activity of 8000 propyl laurate unit g^{-1}) were purchased from Novozymes North America, Inc. (Franklinton, NC, USA). Nitrogen (Ultra High Purity 5.0 Grade) was purchased from the local branch of Airgas, Inc. (Athens, GA, USA). All solvents were of high performance liquid chromatography (HPLC) grade and purchased from local chemical suppliers. All the chemicals were used without further purification.

Enzymatic Transesterification

The transesterification of PG and glycerol was performed in 10 mL reaction vials with an internal cone. After 1 mmol of PG was added into the reaction vials, various amounts of glycerol were added. The reaction mixtures were heated at various temperatures and stirred at 200 rpm under a constant nitrogen flow using a Reacti-Therm™ heating and stirring module (Thermo Fisher Scientific, Waltham, MA, USA) equipped with aluminum heating blocks and a triangular magnetic stirring bar. After PG was dissolved, different percentage loads of Lipozyme® 435 were added relative to the substrate weight. Samples (2 μL) were withdrawn every 24 hours then diluted to 1 mL with methanol for HPLC analysis.

Reaction Mixture Analysis

Samples from the reaction mixture were withdrawn and diluted 10-fold with methanol. Sample aliquots were analyzed by thin layer chromatography (TLC) on 250 μm silica gel G (Uniplate, Analtech, Newark, DE, USA). Separation was achieved using methanol/chloroform (1:3, v/v) as the mobile phase. The TLC plates were directly visualized under 254 nm ultraviolet (UV) light for preparative purposes or after spraying with 0.2% 2′,7′-dichlorofluorescein dissolved in methanol (w/w). The band corresponding to GG on the preparative plates was recovered and extracted with methanol. The solvent was then evaporated under a nitrogen flow and the product was further analyzed using FT-IR and NMR spectroscopy. The Rf values were: glycerol, 0.54; GA, 0.77; GG, 0.66; and PG, 0.96.

The reaction was monitored by HPLC on an Agilent1260 Infinity system (Agilent Technologies, Santa Clara, CA, USA), equipped with a diode-array detector (DAD) scanned at 280 nm and a Sedex 85 low-temperature evaporative light-scattering detector (LT-ELSD) operated at 3.3 bar and 35°C. A reverse phase C18 column (Ultrasphere ODS, 5 μm, 250 × 4.6 mm) was used at a controlled temperature of 35°C and. DAD was used to quantify PG, GA, and GG, whereas LT-ELSD was used to monitor glycerol. Considering that the UV–Vis spectra of PG, GA, and GG were identical, the compounds were quantified using the area normalization method. The separation was achieved by injecting a 20 μL sample at a flow rate of 0.7 mL min^{-1} using a binary eluent as the mobile phase, which consisted of solvent A/water with 1% acetic acid (v/v), and solvent B/methanol. The elution sequence consisted of a linear gradient from 90% (v/v) A to 0% A (v/v) in 30 min, followed by an isocratic elution of solvent B for 10 min. Throughout the whole sequence, the UV spectra

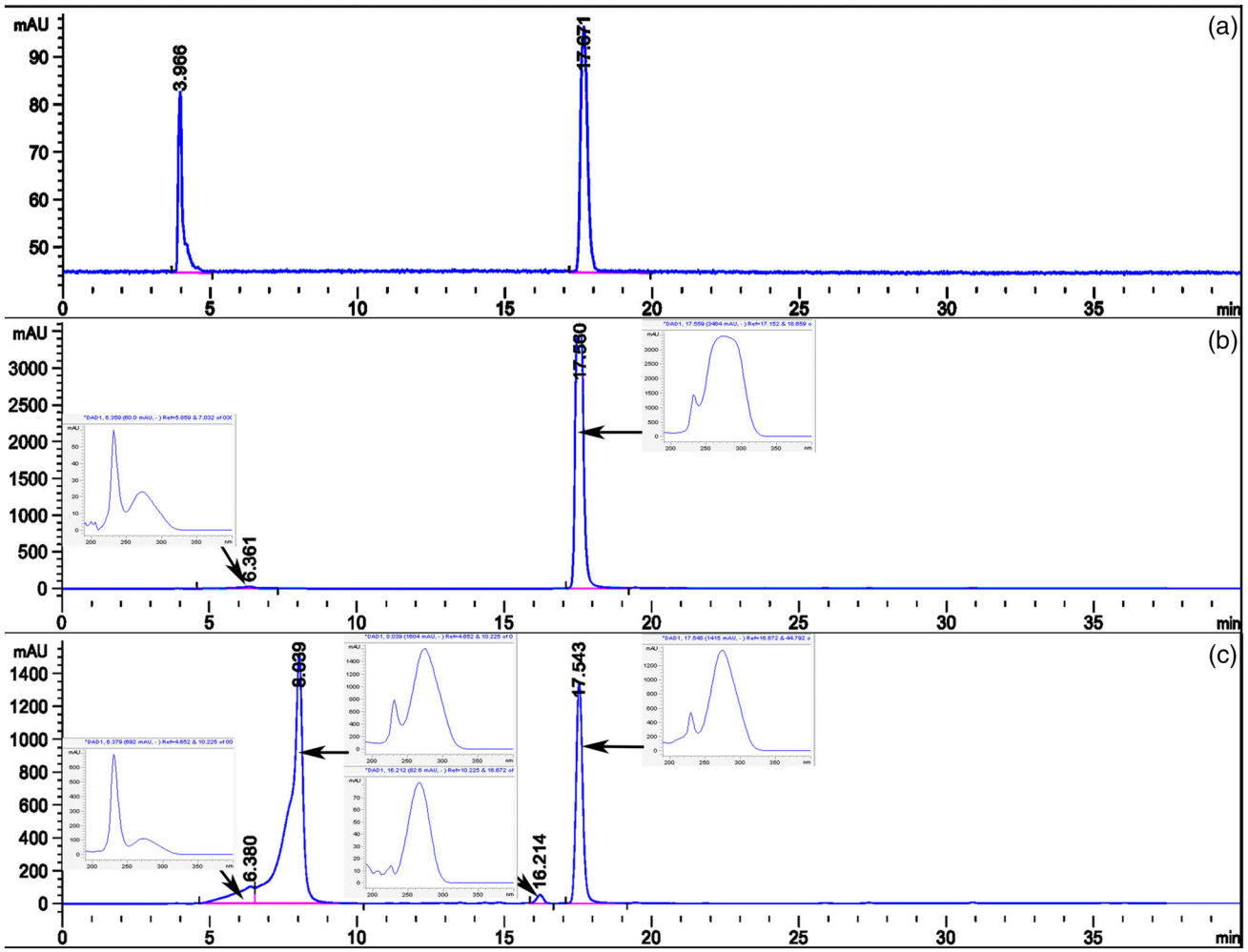

Fig. 1 HPLC results of the reaction mixtures. *Reaction conditions*: 50°C, glycerol/PG = 25:1 (mol/mol), enzyme load 25% (relative to the total weight of the substrates). (a) HPLC-ELSD analysis of the reaction mixture at 0 hour, (b) HPLC-DAD analysis of the reaction mixture at 0 hour with detection at 280 nm, and (c) HPLC-DAD analysis of the reaction mixture at 120 hours with detection at 280 nm

(from 190 to 400 nm) were recorded for analysis of the peak purity. Under these conditions, the retention times were: glycerol, 4.0 min; GA, 6.4 min; GG, 8.0 min; and PG, 17.6 min (Fig. 1). The yield of GG, the conversion of PG, and the hydrolysis rate were calculated according to the following equations:

$$\text{Yield}\,(\%) = \frac{\text{Moles of GG formed}}{\text{Moles of PG at } t = 0\,\text{hour}} \quad (1)$$

$$\text{Conversion}\,(\%) = \frac{\text{Moles of PG consumed}}{\text{Moles of PG at } t = 0\,\text{hour}} \quad (2)$$

$$\text{Hydrolysis}\,(\%) = \frac{\text{Moles of GA formed}}{\text{Moles of PG at } t = 0\,\text{hour}} \quad (3)$$

ESI-HRAM-MS/MS Analysis

Eluted HPLC-DAD peaks were collected and dried under a nitrogen atmosphere. For ESI-HRAM MS/MS analysis, the sample was dissolved in methanol. Analysis was performed by direct infusion in a Thermo Orbitrap Elite mass spectrometer (Thermo Fisher Scientific) with an ESI interface using the negative-ion mode. For MS, the instrument was set to scan from 100 to 1000 mass-to-charge (*m/z*). For tandem MS analysis, collision-induced dissociation was chosen as the fragmentation method, Fourier-transform mass spectrometry spectra were collected from 65 to 500 *m/z*. The capillary temperature was set at 200°C, the source voltage was −2.99 kV, and the vaporizer temperature was 223.80°C.

FT-IR and NMR Analyses

The FT-IR spectra were collected using a Thermo Nicolet Nexus FT-IR 1100 spectrometer (Thermo Fisher Scientific) equipped with an ZnSe attenuated total reflection attachment (ν_{max} is reported in cm^{-1}). After 10 mg of the samples were dissolved in 1 mL methanol, a drop of the solution was placed onto the ZnSe crystal. Spectra were collected after evaporation of the solvent. Spectral data were collected from 500 to 4000 cm^{-1} with a resolution of 4 cm^{-1} and 32 scans. The data were processed using Omnilab software.

For NMR spectroscopy analysis, 10 mg of the sample collected by TLC or HPLC was dissolved in 1 mL deuterium oxide. ^{1}H, ^{13}C, gradient correlation spectroscopy (gCOSY), ^{1}H–^{13}C gradient heteronuclear single-quantum coherence (gHSQC), and ^{1}H–^{13}C gradient heteronuclear multiple bond correlation (gHMBC) spectra were recorded at 25°C using a Varian Mercury-300 (MHz) NMR system (Agilent Technologies) equipped with a 5 mm broad band room temperature probe, and chemical shifts were reported in parts per million (δ/ppm). The chemical shifts were referenced to the residual peak for HDO (δ_H 4.79 ppm) and the acetic acid residual peak ($\delta H/\delta_C$ 2.00/20.2, 175.21 ppm). For ^{1}H NMR analysis, the scan range was set to vary from 0 to 9 ppm with 16 scans. The ^{13}C spectra were obtained indirectly from the gHSQC and gHMBC spectra. For gCOSY, the HDO peak was purged, and the scan range was from 0 to 9 ppm with 800 t1 increments and 4 scans per t1 increment. For gHSQC, the ^{13}C spectrum width ranged from 0 to 160 ppm, and the ^{1}H spectrum width ranged from 0 to 9 ppm with 128 t1 increments and 16 scans per increment. For gHMBC, the ^{13}C spectrum width ranged from 0 to 190 ppm, and the ^{1}H spectrum width ranged from 0 to 9 ppm with 256 t1 increments and 56 scans per increment. The ^{1}H spectra of gHSQC and gHMBC were both acquired at 300 MHz. The ^{13}C spectra of gHSQC and gHMBC were acquired at 75 MHz. The chemical shifts of GG were assigned based on the information from both the 1D and 2D NMR spectra (Fig. 3). ^{1}H NMR (300 MHz, D_2O) δ: 7.04 (2H, s, $H_{8.}$), 4.27–4.14 (2H, m, H_1), 4.12–4.03 (1H, m, H_2), and 3.99–3.70 (2H, m, H_4), ^{13}C NMR (75 MHz, D_2O) δ: 65.72 (C_1), 69.54 (C_2), 62.48 (C_4), 120.41 (C_7), 109.90 (C_8), 144.58 (C_9), 138.32 (C_{11}), and 168.12 (C_6).

Experimental Design and Statistical Analysis

To achieve the highest yield of GG, the effects of four reaction variables, i.e., the reaction temperature (T, °C), substrate ratio (glycerol/PG, mol/mol), enzyme load (percentage of enzyme relative to the total substrate weight), and reaction time (t, hour), were analyzed and optimized using the Taguchi method. An L_{18} (3^4) orthogonal array (Table 1) was adapted from the standard Taguchi method (Taguchi, 1987). As a robust approach for fractional factorial experimental design, the Taguchi method provides an efficient algorithm to find the optimum design for engineering, which allows

Table 1 Experimental design and the effects of the reaction temperature, substrate ratio, reaction time, and enzyme load on the yield of GG, conversion of PG, and hydrolysis

Trials	T (°C)	Substrate ratio	t (hours)	Enzyme load (%)	Yield (%)	Conversion (%)	Hydrolysis (%)
1	50	5	24	5	1.7 ± 1.4	5.4 ± 2.1	2.8 ± 0.5
2	50	15	120	15	41.6 ± 1.6	46.2 ± 2.0	3.7 ± 0.2
3	50	25	72	25	47.2 ± 1.0	53.7 ± 0.9	4.8 ± 0.4
4	65	5	120	25	1.8 ± 0.1	4.5 ± 0.4	2.0 ± 0.8
5	65	15	72	5	9.2 ± 2.2	10.8 ± 2.4	1.4 ± 0.5
6	65	25	24	15	17.1 ± 2.0	19.9 ± 2.5	1.6 ± 0.4
7	80	5	72	15	1.2 ± 0.1	5.3 ± 0.3	3.1 ± 0.2
8	80	15	24	25	13.8 ± 1.6	18.2 ± 2.8	2.7 ± 0.3
9	80	25	120	5	16.7 ± 2.6	17.5 ± 2.0	1.1 ± 0.1
10	50	5	120	5	5.4 ± 2.6	10.3 ± 3.3	4.0 ± 0.9
11	50	15	72	15	29.6 ± 3.1	34.5 ± 3.7	3.9 ± 0.7
12	50	25	24	25	19.9 ± 0.5	23.8 ± 1.2	2.0 ± 0.2
13	65	5	72	25	2.0 ± 0.6	4.6 ± 1.6	1.5 ± 0.3
14	65	15	120	5	11.4 ± 3.4	14.2 ± 4.3	2.0 ± 0.8
15	65	25	72	15	29.7 ± 2.2	34.7 ± 2.7	3.9 ± 0.7
16	80	5	24	15	1.1 ± 0.1	5.1 ± 0.1	2.8 ± 0.1
17	80	15	120	25	14.1 ± 3.5	17.7 ± 3.6	2.1 ± 0.2
18	80	25	72	5	5.6 ± 1.6	6.8 ± 1.8	0.8 ± 0.1

All the results are average of triplicate reactions ± SD.

the reduction of the number of experiments required to optimize a process (Mohan et al., 2009). The reaction temperature (50, 65, and 80°C), substrate ratio (5, 15, and 25), enzyme load (5%, 15%, and 25%), and reaction time (24, 72, 120 hours) were selected based on the reports in the literature involving the use of CALB to catalyze the esterification/transesterification of phenolic acids (Nam et al., 2017; Sun and Hu, 2017). As shown in Table 1, 18 reaction variables were tested (each in triplicate), and each variable was evaluated using an orthogonal design.

Statistical analysis of the experimental results was performed using JMP® software (version 13.2.0, SAS Institute, Inc., Cary, NC, USA). The results were expressed as mean values ± SD. To determine the optimal reaction conditions and evaluate the effects of the reaction variables, the yield of GG and the signal-to-noise ratio (S/N, dB) were analyzed by ANOVA with 2-way interactions. The results were expressed as least-squares means (LS mean) ± SEM. Tukey's honest significant difference test (Tukey HSD) and the LSD test were used to determine the differences that occurred when varying each reaction parameter and the level of significance ($P < 0.05$). The S/N ratio is a measure of the robustness that can be used to detect the control factor settings for a minimum impact of noise on a response (Willett and Akoh, 2018). The larger the S/N is, the higher the yield, as shown in Eq. 4.

$$\mathrm{S/N\,(dB)} = -10\log\left(\frac{1}{n}\sum_{i=1}^{n} y_i^{-2}\right) \quad (4)$$

in which y_i represents the experimental value of the ith experiment and n represents the number of replications.

The experimental results were also analyzed by regression analysis using a polynomial quadratic equation to correlate each response variable with the independent variables, using Eq. 5:

$$Y = \beta_0 + \sum_{i=1}^{4}\beta_i X_i + \sum_{i=1}^{4}\beta_{ii} X_i^2 + \sum_{i=1}^{4}\sum_{j=1}^{4}\beta_{ij} X_i X_j \quad (5)$$

in which Y is the predicted response, X_i and X_j are independent factors, β_0 is the intercept, β_i is the linear coefficient, β_{ii} is the quadratic coefficient, and β_{ij} is the interaction coefficient.

To select the model with the best fit, the forward stepwise minimum Bayesian information criterion (BIC) parameter/model selection method was used. The analyses were performed using three-dimensional diagrams constructed for the selected model. The ANOVA test, level of significance ($P < 0.05$), and statistically fitting (R^2) were used to evaluate the model. Time-course reactions were also used for model validation.

Results and Discussion

Structural Characterization of GG

The alcoholysis of PG with glycerol (Scheme 1) was performed in an open system under a nitrogen flow in a solvent-free system, catalyzed with an immobilized and commercially available food-grade lipase (Lipozyme® 435). The HPLC and spectra of the reaction mixture detected by DAD and/or ELSD at the start and at the end of reaction are shown in Fig. 1. During the course of the reaction, a decrease in the PG and the formation of GG were observed. The same UV absorption peak was observed at 275 nm for PG, GG, and GA, which agreed with the previous data (Artamonov et al., 1999). Notably, there was a small peak with a retention time of 16.2 min that also had the same UV absorption pattern (Fig. 1c), indicating that it may have been glyceryl digallate.

The GG product was further characterized using FT-IR, ESI-HRAM-MS/MS, and NMR spectroscopy. A broad band within 3100–3700 cm^{-1} region typical of the O–H stretching mode of the hydroxy was observed in the FT-IR spectrum (spectra not shown). This was ascribed to the unesterified hydroxyl groups of the glycerol moiety and hydroxyl group in the gallate part of the molecule following formation of the ester function. The peak at 1699 cm^{-1} indicated the existence of the ester linkage in GG, which shifted from the typical signal at 1740 cm^{-1} owing to the influence of the aromatic ring. A sharp signal at 1610 cm^{-1} indicated the existence of an aromatic structure bearing hydroxyl groups in the ortho positions, which was consistent with the arrangement of the hydroxyl groups in GG. The presence of a pair of sharp bands at 1208 and 1137 cm^{-1} indicated the asymmetrical C–O of the ester linkage.

ESI-HRAM-MS/MS analysis was used to determine the elemental composition and structure of the new compounds (Fig. 2). In MS^1, the molecular ion $[M\text{-}H]^{-1}$ peak found at 243.0508 *m/z* was consistent with $C_{10}H_{14}0_7$ as the chemical formula for the molecular ion (calculated 243.0510 *m/z*, error = −0.82 ppm). The tandem ESI-HRAM-MS data (generated in the negative-ion mode) showed an $[M\text{-}H]^{-1}$ peak at 243.0510 *m/z* (calculated 243.0510 *m/z*, error = 0 ppm). In MS^2, the most abundant fragment generated from the molecular ion was 169.0144 *m/z*, which was attributed to a GA molecule with one hydrogen atom lost (calculated 169.0142 *m/z*, error = 1.18 ppm), confirming bond formation between GA and glycerol. Other less abundant peaks could also be found from GG by the loss of logical neutral species (Fig. 2). As shown in Fig. 2, the MS^2 results confirmed the structure of the product and demonstrated that the final compound generated by enzymatic esterification was GG. However, the ESI-HRAM-MS/MS

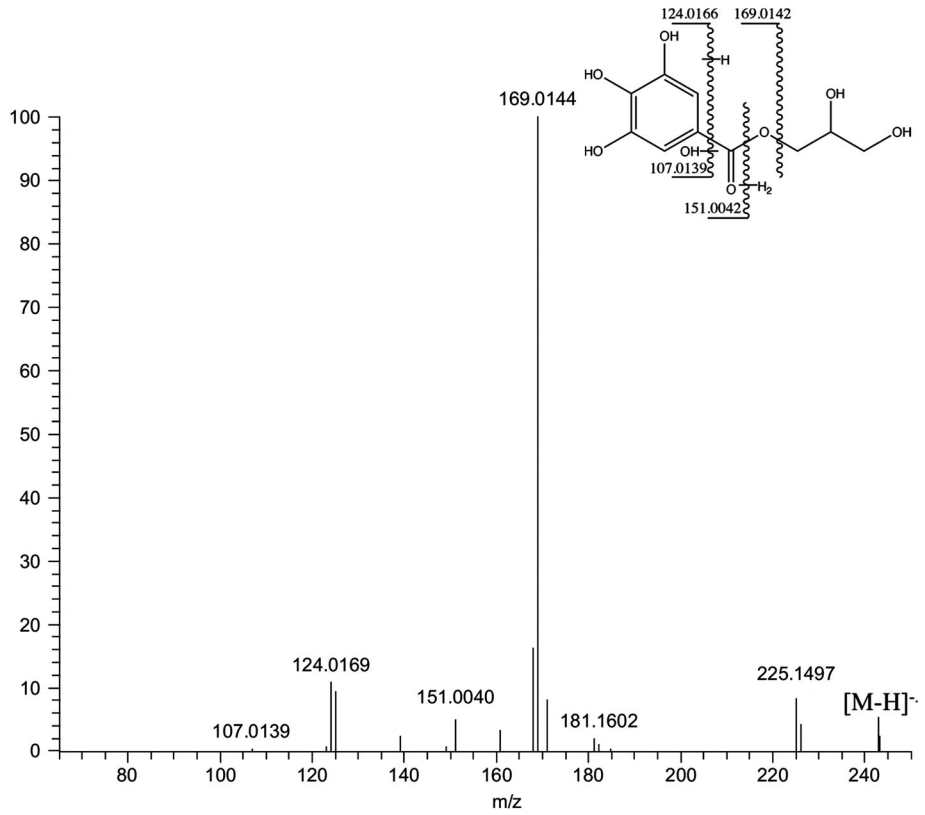

Fig. 2 ESI-HRAM-MS/MS analysis of GG

results could not confirm the position of the ester function on the glycerol moiety of GG.

The results of the ^{1}H- and ^{13}C-unidimensional NMR together with 2D gCOSY, gHSQC, and HMBC NMR provided evidence that the primary hydroxyl group of glycerol was esterified and formed a linkage with the GA moiety. The ^{1}H spectrum (Fig. 3a) showed that five hydrogen atoms from the glycerol moiety had three different chemical shifts, which indicated that the formed ester had an asymmetrical structure. Furthermore, only two hydrogen atoms were attached to the benzene ring, and these two hydrogens had the same chemical shift in the ^{1}H NMR spectrum, which confirmed the structure of the esterified GA moiety. The results of gCOSY NMR unveiled the connectivity of the hydrogen atoms, providing additional evidence of the hydrogen arrangement of GG (Fig. 3b). The ^{13}C NMR results indicated that the three carbon atoms of the glycerol moiety had three different chemical shifts, which provided further evidence that the formed ester had an asymmetrical structure. The gHSQC spectra (Fig. 3c) displayed the one-bond correlation of the carbon atoms and hydrogen atoms in the GG molecule. Combined with the information obtained by ^{1}H NMR spectroscopy, the carbon atoms of the glycerol moiety were of particular interest. Results showed that both C1 and C4 had two protons attached directly, while only one proton was directly attached to C2. Furthermore, C1 and C4 showed different chemical shifts, which indicates the ester linkage was formed at the primary hydroxyl group of the glycerol moiety. Assuming the ester linkage had formed at the C2 hydroxy, the chemical shifts of C1 and C4 would be the same. The gHMBC experiments were used to investigate the long-range coupling between carbon atoms and proton atoms. Fig. 3d shows the results acquired by gHMBC experiment configured for an 8-Hz coupling. The long-range correlations acquired from this experiment, particularly between the carbonyl group and H1, were consistent with the ester linkage of GG formed at the primary hydroxyl group of the glycerol moiety. Regarding the 1D NMR and 2D NMR data of the product, our data indicated that when using Lipozyme® 435 as a biocatalyst, GA was esterified only on the primary hydroxyl group of glycerol.

Taguchi Method

The mean values of the yield, conversion, and hydrolysis were calculated according to Eqs. 1–3, respectively. The S/N ratios were calculated using the method of "larger is

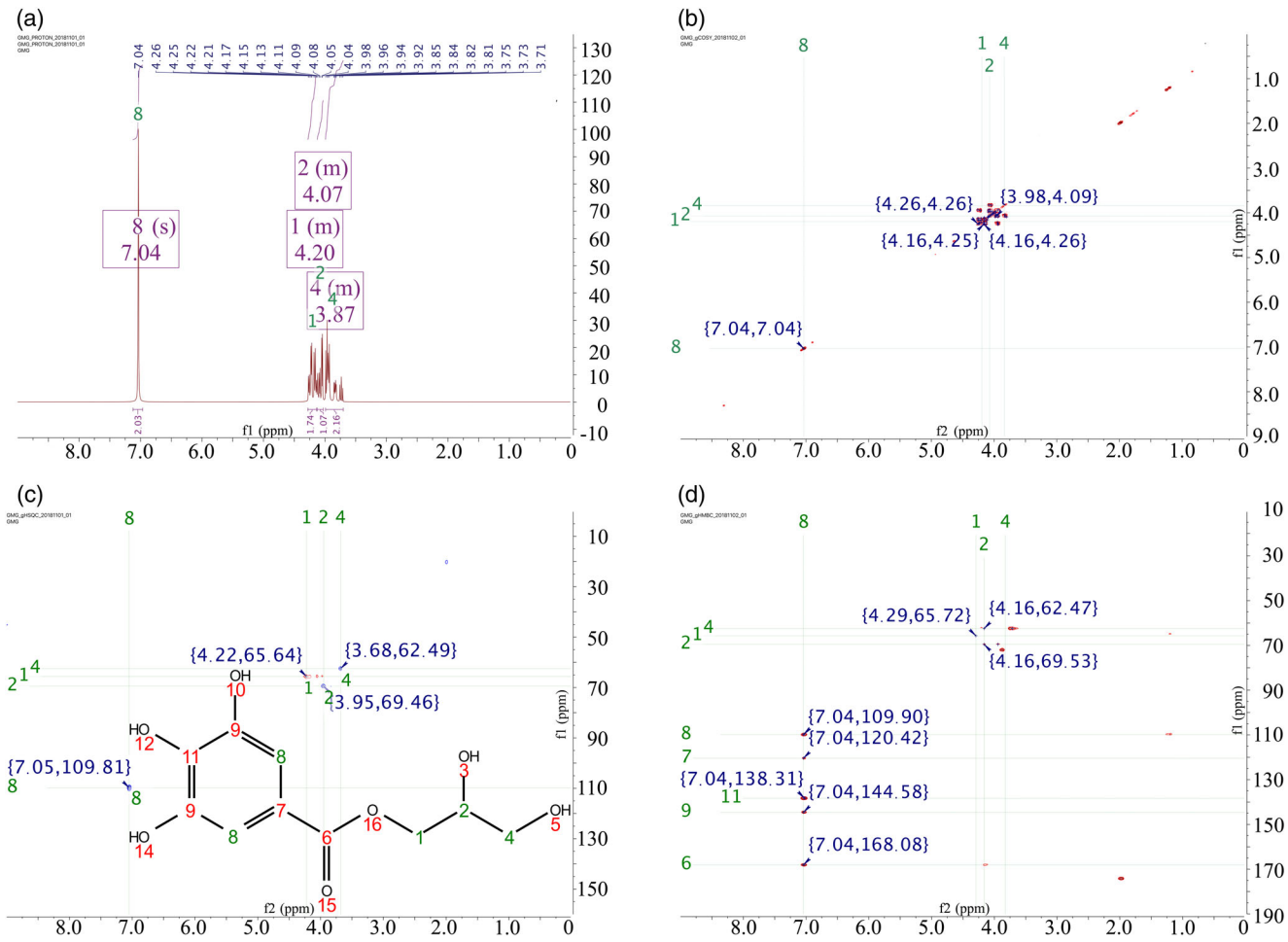

Fig. 3 NMR spectra and chemical shift assignment of GG: (a) ^{1}H NMR spectrum, (b) gCOSY spectrum, (c) gHSQC spectrum, and (d) gHMBC spectrum

the better" in Eq. 4. For all 18 experimental combinations described in Table 1, each condition was repeated trice. Because the experimental design was orthogonal, all specified parameters could be estimated independent of any other. Therefore, the effects of each factor were separated out in terms of the S/N together with the mean response, reported in LS means ± SEM (Fig. 4).

Effect of Reaction Temperature

As shown in Fig. 4a, both the yield and S/N were the highest at 50°C, whereas the yield at 60°C was significantly higher than the yield at 80°C, which indicated that the yield of GG decreased with increasing temperature from 50 to 80°C. The highest LS mean for the yield (31.3 ± 1.0%) and S/N (29.7 ± 1.7 dB) were obtained at 50°C. The results could be explained by partial thermal deactivation of the enzyme at the higher temperatures. In addition, the yield of GG and S/N in this range of temperature tested fits quadratic trendlines with *R*-values equal to 1, suggesting the effect of temperature could be fitted into a quadratic model. To investigate the yield at lower temperature, time-course reactions were performed at 35, 40, 45, and 50°C, with other conditions optimized (enzyme load of 23.8%, substrate ratio of 25). As shown in Fig. 5a, lower conversions were obtained at 35, 40, and 45°C after reaction for 120 hours, which was compatible with the Arrhenius law. An increased yield could also result from a decrease in the viscosity in the reaction medium and, consequently, from the reduction of mass transfer resistances. Considering the above data, 50°C was selected as the optimum reaction temperature.

Effect of the Substrate Ratio

The highest LS mean yield (31.8 ± 1.7%) and S/N (30.3 ± 1.0 dB) were obtained at a 25:1 (glycerol/PG, mol/mol) substrate ratio. As shown in Fig. 4b, when the

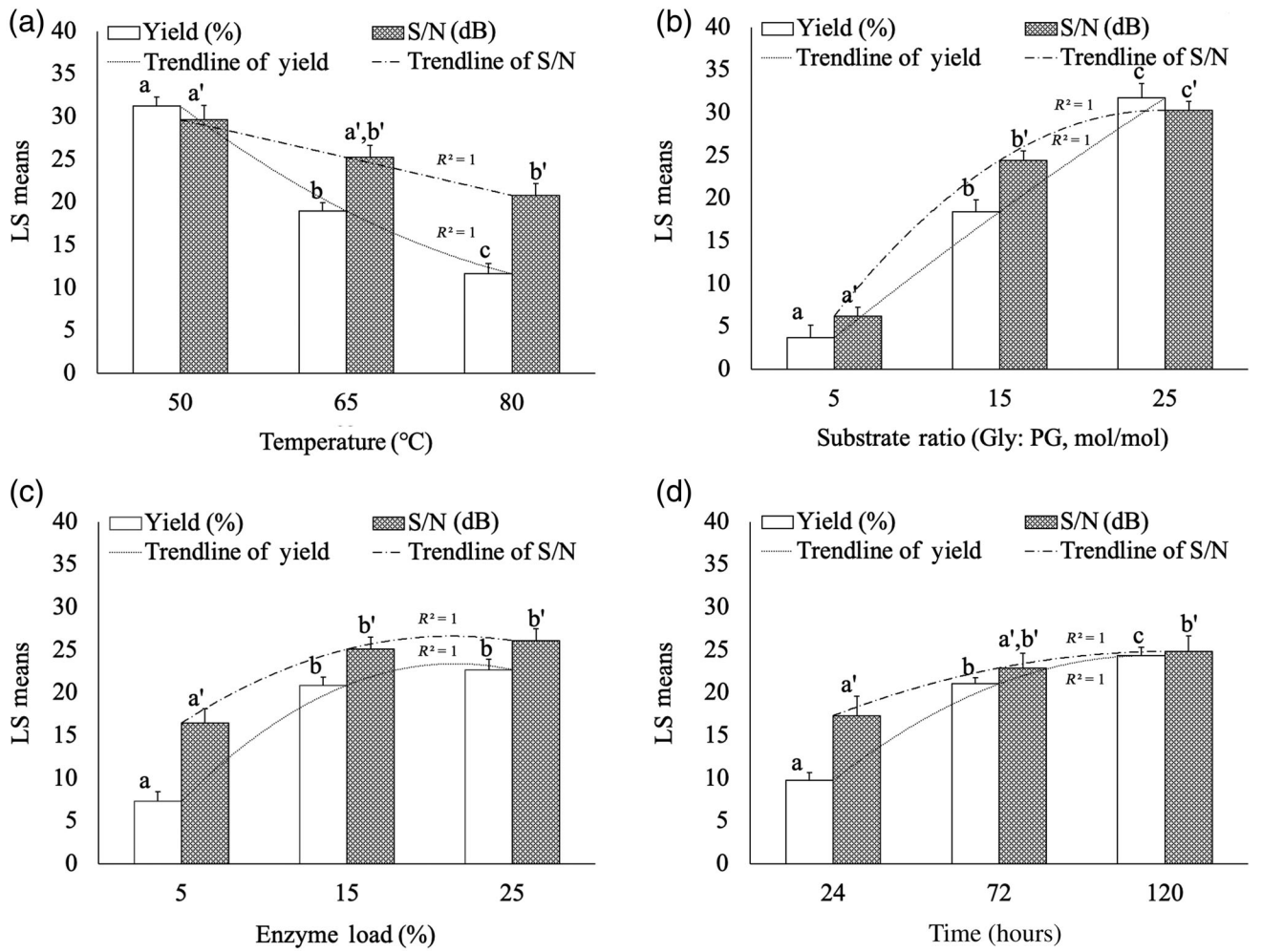

Fig. 4 Effects of the (a) reaction temperature on yield, (b) substrate ratio on yield, (c) enzyme load on yield, and (d) reaction time on yield. Different letters indicate significant difference at $P < 0.05$ with Tukey's HSD and LSD tests

substrate ratio of glycerol to PG reduced from 25:1 to 15:1 or 5:1, both the yield of GG and S/N significantly decreased. These results showed that increasing the proportion of glycerol improved the conversion rate of PG, which could be accredited to the excessive amount of glycerol serving as a reactant and reaction medium for the reaction. Notably, hydrolysis increased when increasing the substrate ratio (data not shown). Therefore, 25:1 glycerol/PG (mol/mol) was chosen as the optimum reaction substrate ratio. Similar to the effect of temperature, the GG yield and S/N in the range of substrate ratios tested fit quadratic trendlines with R-values equal to 1, suggesting that the effect of varying the substrate ratio could be fitted into a quadratic model.

Effect of Enzyme Load

The highest LS mean of yield and S/N were obtained at 25% enzyme load of total substrates (w/w), 22.7 ± 1.2% and 26.1 ± 1.4 dB, respectively. As shown in Fig. 4c, when the enzyme load decreased from 25% to 5%, both the yield of GG and S/N significantly decreased. Although the LS mean yield and S/N were significantly higher at 25%, the difference between 15% enzyme load and 25% enzyme load was not significant. Furthermore, similar to the effect of the temperature/substrate ratio, the GG yield and S/N ratio in the tested range of enzyme load fit quadratic trendlines with R-values equal to 1, suggesting that the effect of the enzyme load could be fitted into a quadratic model. However, the trendlines of yield and S/N suggest that a point exists between a 25% and 15% enzyme load with a higher yield and S/N ratio. Thus, an optimal enzyme load of 23.8% was predicted by regression analysis. The three levels of enzyme loads (15%, 23.8%, and 25%) were tested in time-course reactions in triplicate (with the other conditions optimized) to determine the optimal enzyme load (Fig. 5b). The results showed that the highest yield

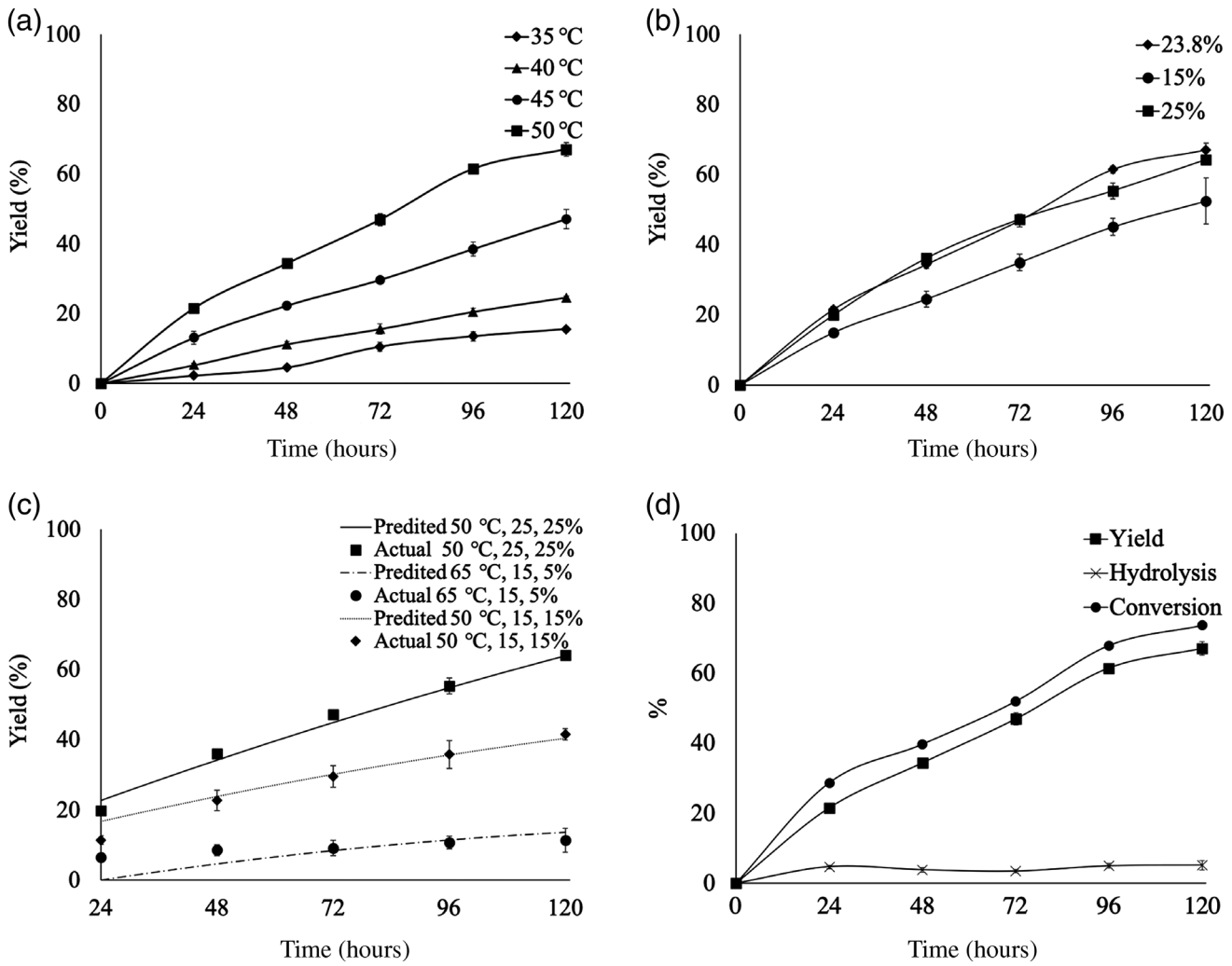

Fig. 5 Time-course reactions under different conditions: (a) low temperature (*fixed-reaction conditions*: glycerol/PG = 25:1, and enzyme load 23.8%), (b) three levels of enzyme load (fixed-reaction conditions: 50°C, glycerol/PG = 25:1), (c) validation of the proposed model (the reaction conditions listed are the reaction temperature, substrate ratio, and enzyme load, respectively), and (d) under the optimal conditions (50°C, glycerol/PG = 25:1, enzyme load 23.8%)

was achieved with an enzyme load of 23.8%, which was selected as the optimal enzyme load. The decreased yield and S/N ratio at a high enzyme concentration could be explained by enzyme aggregation (Sun and Hu, 2017).

Effect of Reaction Time

The highest LS mean yield (24.4 ± 1.0%) and S/N (24.9 ± 1.8 dB) were obtained at a 120-hour reaction time. As shown in Fig. 4d, when the reaction time decreased from 120 to 72 hours or 24 hours, both the yield of GG and S/N significantly decreased. Considering that hydrolysis increased with an increasing reaction time (data not shown), and to prevent the conversion of monoesters to diesters, 120 hours was chosen as the optimum reaction time. Similar to the effect of temperature, the yield of GG and S/N in the tested range of reaction time fits quadratic trendlines with R-values equal to 1, suggesting that the effect of the reaction time could be fitted to a quadratic model.

Regression Analysis and Determination of Optimal Conditions

Based on the characteristics of the effects of four factors, a polynomial quadratic model with two-way interactions was selected, as described in Eq. 5. The coefficients of the proposed model were calculated based on the experimental responses. The fitted model that is expressed in coded variables is represented by Eq. 6:

Table 2 ANOVA results observed when fitting the experimental data to the proposed model

Source	Degree of freedom	Sum of squares	Mean square	*F*-value	*P*-value
Model	10	9830.10	983.01	126.29	<0.0001*
Residual	43	334.70	7.78		
Total	53	10,164.81			
Root mean square error (RMSE) = 2.7899, R^2 = 0.9671					

*Statistically significant at 99.99% of confidence level.

$$\begin{aligned}\text{Yield}\,(\%) = &-12.3628 - 0.0247X_1 + 0.2184X_2 \\ &+ 0.4272X_3 + 2.0673X_4 - 0.0279X_2^2 - 0.0007X_3^2 \\ &- 0.0635X_4^2 - 0.0070X_1X_3 + 0.0182X_2X_3 \\ &+ 0.0383X_2X_4 \qquad (6)\end{aligned}$$

in which X_1 is the reaction temperature (°C), X_2 is the substrate ratio (glycerol/PG, mol/mol), X_3 is the reaction time (hours), and X_4 is the enzyme load (%).

The quality of the fitted model was confirmed by ANOVA, as demonstrated in Table 2. As shown in Table 2, the sum of squares related to the regression was statistically significant when using the *F*-test at a 99.99% probability level, which suggested that the variation accounted for by the model was significantly greater than the residual variation. There was less than a 0.01% probability that the model F-value could occur owing to noise. Likewise, the coefficient (R^2) of the regression model indicated that over 96.7% of the variability in the response could be explained by the predicted second-order polynomial equation given above. An accuracy check is necessary to generate an adequate model. In this respect, the validity of the model was established by comparing the experimental results obtained with three time-course reactions (each reaction performed in triplicate) with the predicted values (Fig. 5c). The actual yields fell within the 95% confidence intervals of the predicted yields. These results confirmed the validity of the model.

The mutual effects of the reaction temperature, substrates ratio, reaction time, and enzyme load on the yield of GG were also illustrated in the three-dimensional diagrams (Fig. 6). The effects of reaction conditions shown in these figures are consistent with the results obtained from the Taguchi method. Combining the results of the three-dimensional diagrams with the results obtained in the previous sections, the optimal

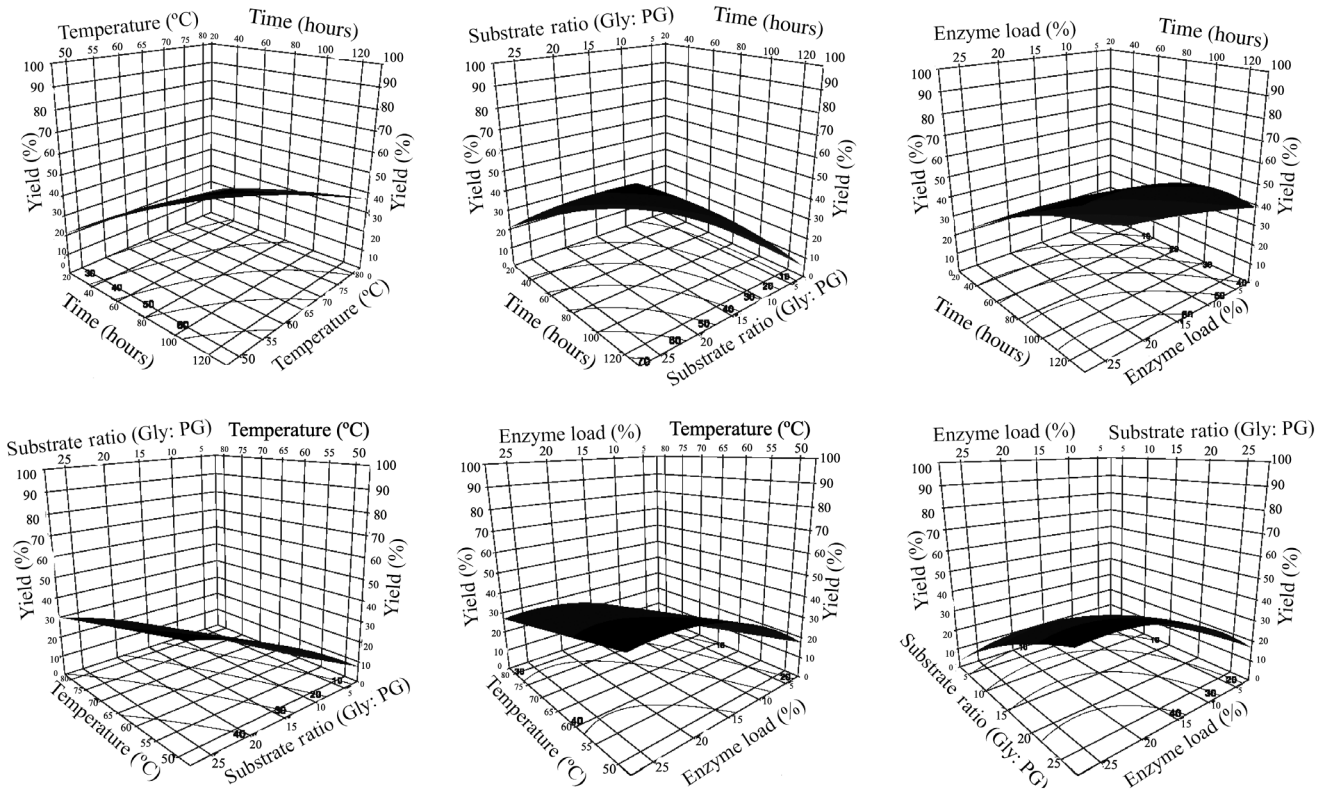

Fig. 6 Three-dimensional diagrams showing the effects of two parameters (as indicated) on the GG yield. For each plot, the other two factors were fixed under the optimal conditions. The optimal reaction conditions were a temperature of 50°C, a glycerol/PG = 25:1 (mol/mol), an enzyme load of 23.8% (relative to the total weight of the substrates), and a reaction time of 120 hours

Table 3 Alcoholysis of PG and glycerol catalyzed by different lipases

Time (hours)	Yield (%)			
	Lipozyme® RM IM[a]	Lipozyme® TL IM[a]	Novozym® 435[a]	Lipozyme® 435 in *t*-butanol
24	ND	ND	23.7 ± 3.7	0.2 ± 0.1
48	ND	ND	42.2 ± 1.5	0.3 ± 0.1
72	ND	ND	57.2 ± 5.2	0.4 ± 0.1
96	ND	ND	72.5 ± 5.9	0.5 ± 0.1
120	ND	ND	75.0 ± 2.5	0.5 ± 0.1

All results are average of triplicate reactions ± SD.

ND, not detected.

[a] Reactions were carried out without using extra solvent.

conditions were determined to be: 23.8% enzyme load relative to the total substrates (w/w), substrate ratio glycerol/PG = 25:1 (mol/mol), a reaction temperature of 50°C, and a reaction time of 120 hours. The actual yield of GG, conversion of PG, and the hydrolysis rate were confirmed by a time-course reaction in triplicate under the optimal conditions. The results are illustrated in Fig. 5d. After a reaction time of 120 hours, the yield of GG was 67.1 ± 1.9%, the conversion of PG was 73.6 ± 1.5%, and the hydrolysis rate was 5.1 ± 1.3%. According to the model, the predicted optimal yield was 59.9–69.2%, which agreed with the actual yield. The good agreement between the actual and predicted values validated the model.

Other Lipases and Solvent Medium

Lipozyme® RM IM, Lipozyme® TL IM, and Novozym® 435 were used separately as catalysts under the same reaction conditions determined in the previous section. As shown in Table 3, the highest yield was achieved using Novozym® 435 as the catalyst, while no GG formation was observed when using Lipozyme® RM IM or Lipozyme® TL IM, indicating that these two lipases are not suitable for catalyzing this reaction. Previous studies with phenolic acids/esters as substrates showed that only CALB could catalyze the reaction with alcohols in moderate to good yields (Buisman et al., 1998), which is in agreement with the results obtained in this work. Although the yield achieved using Novozym® 435 (75.0 ± 2.5%) was higher than the one obtained using Lipozyme® 435 (67.1 ± 1.9%), it should be noted that Novozym® 435 is not a food-grade enzyme. Therefore, Lipozyme® 435 would be a better choice to synthesize GG for applications in food, cosmetic, and pharmaceutical fields.

To check the potential influence of extra solvent in the medium, the reaction was also carried out in 10 mL *t*-butanol using the values previously optimized for the rest of the variables. When using CALB (Lipozyme® 435) in nonaqueous media, the use of hydrophobic solvents generally results in a higher product yield and conversion (Buisman et al., 1998; Figueroa-Espinoza and Villeneuve, 2005). However, the solubilities of PG and glycerol are rather low in apolar solvents. t-Butanol has the highest log P value (0.839) among the solvents that could sufficiently dissolve the substrates (PG and glycerol). After 120 hours of reaction, less than 1.0% product yield was obtained (Table 3). This could be attributed to enzyme deactivation by t-butanol. Similar results were also found in a previous study, where higher yields were observed in a solvent-free system when using CALB as a catalyst for the esterification of cinnamic acid derivatives and aliphatic alcohols (Stamatis et al., 1999).

Conclusion

A novel method for synthesizing GG by the enzymatic transesterification of PG and glycerol was established. GG was synthesized using an immobilized commercially available food-grade lipase, Lipozyme® 435, in a solvent-free system at atmospheric pressure under a nitrogen flow. High PG conversion and GG yield with low hydrolysis were obtained under the optimized conditions. Compared with chemical synthesis of GG, the enzymatic strategy does not require the presence of a strong acid or base as the catalyst (Artamonov et al., 1999; Nonaka and Nishioka, 1983; Song and Xiao, 1988). In this study, we confirmed that the enzymatic preparation of galloylated structured lipids was feasible, and that a green and efficient enzymatic method for the production of GG was developed. This product (GG) may have potential for use as an antioxidant and an active ingredient in the food, cosmetic, and pharmaceutical fields.

Acknowledgments The authors would like to thank Food Science Research, the University of Georgia for supporting this work. Special thanks go to Dr. Dennis R. Phillips and Dr. Chau-Wen Chou from the UGA PAMS facility for assistance with MS analysis, and Dr. John Glushka from the CCRC NMR spectroscopy facility of UGA for assisting NMR analysis.

Conflict of Interest The authors declare that they have no conflicts of interest.

References

Artamonov, A., Nigmatullina, F., Aldabergenova, M., & Dzhiembaev, B. Z. (1999) Synthesis of α-monoglycerides of aromatic acids. *Chemistry of Natural Compounds*, **35**:404–408.

Buisman, G., Van Helteren, C., Kramer, G., Veldsink, J., Derksen, J., & Cuperus, F. (1998) Enzymatic esterifications of functionalized phenols for the synthesis of lipophilic antioxidants. *Biotechnology Letters*, **20**:131–136.

Compton, D. L., Laszlo, J. A., & Berhow, M. A. (2000) Lipase-catalyzed synthesis of ferulate esters. *Journal of the American Oil Chemists' Society*, **77**:513–519.

Compton, D. L., Laszlo, J. A., & Evans, K. O. (2012) Antioxidant properties of feruloyl glycerol derivatives. *Industrial Crops and Products*, **36**:217–221.

Daneshfar, A., Ghaziaskar, H. S., & Homayoun, N. (2008) Solubility of gallic acid in methanol, ethanol, water, and ethyl acetate. *Journal of Chemical & Engineering Data*, **53**:776–778.

EFSA Panel on Food Additives and Nutrient Sources Added to Food (ANS). (2014) Scientific opinion on the re-evaluation of propyl gallate (E 310) as a food additive. *EFSA Journal*, **12**:3642–3688.

Figueroa-Espinoza, M. C., Laguerre, M., Villeneuve, P., & Lecomte, J. (2013) From phenolics to phenolipids: Optimizing antioxidants in lipid dispersions. *Lipid Technology*, **25**:131–134.

Figueroa-Espinoza, M. C., & Villeneuve, P. (2005) Phenolic acids enzymatic lipophilization. *Journal of Agricultural and Food Chemistry*, **53**:2779–2787.

Gamboni, S. E., Palmer, A. M., & Nixon, R. L. (2013) Allergic contact stomatitis to dodecyl gallate? A review of the relevance of positive patch test results to gallates. *Australasian Journal of Dermatology*, **54**:213–217.

Hollande, L., Domenek, S., & Allais, F. (2018) Chemo-enzymatic synthesis of renewable sterically-hindered phenolic antioxidants with tunable polarity from lignocellulose and vegetal oil components. *International Journal of Molecular Sciences*, **19**:3358–3370.

Locatelli, C., Filippin-Monteiro, F. B., & Creczynski-Pasa, T. B. (2013) Alkyl esters of gallic acid as anticancer agents: A review. *European Journal of Medicinal Chemistry*, **60**:233–239.

Masoud, M. S., Hagagg, S. S., Ali, A. E., & Nasr, N. M. (2012) Synthesis and spectroscopic characterization of gallic acid and some of its azo complexes. *Journal of Molecular Structure*, **1014**:17–25.

Mohan, S. V., Raghavulu, S. V., Mohanakrishna, G., Srikanth, S., & Sarma, P. (2009) Optimization and evaluation of fermentative hydrogen production and wastewater treatment processes using data enveloping analysis (DEA) and Taguchi design of experimental (DOE) methodology. *International Journal of Hydrogen Energy*, **34**:216–226.

Nam, S. H., Park, J., Jun, W., Kim, D., Ko, J.-A., El-Aty, A. A., … Yang, K. Y. (2017) Transglycosylation of gallic acid by using Leuconostoc glucansucrase and its characterization as a functional cosmetic agent. *AMB Express*, **7**:224–234.

Nayeem, N., & Smb, A. (2016) Gallic acid: A promising Lead molecule for drug development. *Journal of Applied Pharmacy*, **8**: 213–216.

Nonaka, G., & Nishioka, I. (1983) Tannins and related compounds. X. Rhubarb (2): Isolation and structures of a glycerol gallate, gallic acid glucoside gallates, galloylglucoses and isolindleyin. *Chemical and Pharmaceutical Bulletin*, **31**:1652–1658.

Otto, R. T., Scheib, H., Bornscheuer, U. T., Pleiss, J., Syldatk, C., & Schmid, R. D. (2000) Substrate specificity of lipase B from *Candida antarctica* in the synthesis of arylaliphatic glycolipids. *Journal of Molecular Catalysis B: Enzymatic*, **8**:201–211.

Pion, F., Reano, A. F., Ducrot, P. H., & Allais, F. (2013) Chemo-enzymatic preparation of new bio-based bis-and trisphenols: New versatile building blocks for polymer chemistry. *RSC Advances*, **3**: 8988–8997.

Puppala, M., Ponder, J., Suryanarayana, P., Reddy, G. B., Petrash, J. M., & LaBarbera, D. V. (2012) The isolation and characterization of β-glucogallin as a novel aldose reductase inhibitor from *Emblica officinalis*. *PLoS One*, **7**:e31399.

Ravelo, M., Esteban, J., Ladero, M., & García-Ochoa, F. (2016) Enzymatic synthesis of ibuprofen monoglycerides catalyzed by free *Candida antarctica* lipase B in a toluene–glycerol biphasic medium. *RSC Advances*, **6**:69658–69669.

Roby, M. H. H. (2017) Synthesis and characterization of phenolic lipids. In M. Soto-Hernández, M. P. Tenango, & R. García-Mateos (Eds.), *Phenolic compounds-natural sources, importance and applications* (pp. 89–116). London, England: InTech.

Song, Z., & Xiao, Z. (1988) The preparation of 1-glycerol Gallate and study on its Antioxidantion properties. *Chemistry and Industry of Forest Products*, **3**:9–18.

Stamatis, H., Sereti, V., & Kolisis, F. (1999) Studies on the enzymatic synthesis of lipophilic derivatives of natural antioxidants. *Journal of the American Oil Chemists' Society*, **76**:1505–1510.

Sun, S., & Hu, B. (2017) A novel method for the synthesis of glyceryl monocaffeate by the enzymatic transesterification and kinetic analysis. *Food Chemistry*, **214**:192–198.

Sun, S., Hu, B., Qin, F., & Bi, Y. (2015) Comparative study of soybean oil and the mixed fatty acids as acyl donors for enzymatic preparation of feruloylated acylglycerols in ionic liquids. *Journal of Agricultural and Food Chemistry*, **63**:7261–7269.

Taguchi, G. (1987) *System of experimental design: Engineering methods to optimize quality and minimize costs* (Vol. **1**). White Plains, NY: UNIPUB/Kraus International.

Tamayo, J., Ladero, M., Santos, V., & Garcia-Ochoa, F. (2012) Esterification of benzoic acid and glycerol to α-monobenzoate glycerol in solventless media using an industrial free *Candida antarctica* lipase B. *Process Biochemistry*, **47**:243–250.

Ter Veld, M. G., Schouten, B., Louisse, J., van Es, D. S., van der Saag, P. T., Rietjens, I. M., & Murk, A. J. (2006) Estrogenic potency of food-packaging-associated plasticizers and antioxidants as detected in ERα and ERβ reporter gene cell lines. *Journal of Agricultural and Food Chemistry*, **54**:4407–4416.

Willett, S. A., & Akoh, C. C. (2018) Application of Taguchi method in the enzymatic modification of menhaden oil to incorporate capric acid. *Journal of the American Oil Chemists' Society*, **95**:299–311.